Astronomy & Astrophysics manuscript no. 14720
May 31, 2010
© ESO 2010

Letter to the Editor

The Hα line forming region of AB Aur spatially resolved at sub-AU with the VEGA/CHARA spectro-interferometer

K. Perraut[1], M. Benisty[2], D. Mourard[3], S. Rajabi[2,4], F. Bacciotti[2], Ph. Bério[3], D. Bonneau[3], O. Chesneau[3], J.M. Clausse[3], O. Delaa[3], A. Marcotto[3], A. Roussel[3], A. Spang[3], Ph. Stee[3], I. Tallon-Bosc[5], H. McAlister[6,7], T. ten Brummelaar[6], J. Sturmann[6], L. Sturmann[6], N. Turner[6], C. Farrington[6] and P.J. Goldfinger[6]

[1] Laboratoire d'Astrophysique de Grenoble (LAOG), Université Joseph-Fourier, UMR 5571 CNRS, BP 53, 38041 Grenoble Cedex 09, France
[2] INAF-Osservatorio Astrofisico di Arcetri, Largo E. Fermi 5, 50125 Firenze, Italy
[3] Laboratoire Fizeau, OCA/UNS/CNRS UMR6525, Parc Valrose, 06108 Nice cedex 2, France
[4] Centro de Astrofisica, Universidade do Porto, 4150-752 Porto, Portugal
[5] Université de Lyon, Lyon, F-69003, France; Université Lyon 1, Observatoire de Lyon, 9 avenue Charles André, Saint Genis Laval, F-69230; CNRS, UMR 5574, Centre de Recherche Astrophysique de Lyon; Ecole Normale Supérieure, Lyon, F-69007, France
[6] Georgia State University, P.O. Box 3969, Atlanta GA 30302-3969, USA
[7] CHARA Array, Mount Wilson Observatory, 91023 Mount Wilson CA, USA

Received ...; accepted ...

ABSTRACT

Context. A crucial issue in star formation is to understand the physical mechanism by which mass is accreted onto and ejected by a young star. To derive key constraints on the launching point of the jets and on the geometry of the winds, the visible spectro-polarimeter VEGA installed on the CHARA optical array can be an efficient means of probing the structure and the kinematics of the hot circumstellar gas at sub-AU.

Aims. For the first time, we observed the Herbig Ae star AB Aur in the Hα emission line, using the VEGA low spectral resolution (R=1700) on two baselines of the array.

Methods. We computed and calibrated the spectral visibilities of AB Aur between 610 nm and 700 nm in spectral bands of 20.4 nm. To simultaneously reproduce the line profile and the inferred visibility around Hα, we used a 1-D radiative transfer code (RAMIDUS/PROFILER) that calculates level populations for hydrogen atoms in a spherical geometry and that produces synthetic spectro-interferometric observables.

Results. We clearly resolved AB Aur in the Hα line and in a part of the continuum, even at the smallest baseline of 34 m. The small P-Cygni absorption feature is indicative of an outflow but could not be explained by a spherical stellar wind model. Instead, it favors a magneto-centrifugal X-disk or disk-wind geometry. The fit of the spectral visibilities from 610 to 700 nm could not be accounted for by a wind alone, so another component inducing a visibility modulation around Hα needed to be considered. We thus considered a brightness asymmetry possibly caused by large-scale nebulosity or by the known spiral structures.

Conclusions. Thanks to the unique capabilities of VEGA, we managed to simultaneously record for the first time a spectrum at a resolution of 1700 and spectral visibilities in the visible range on a target as faint as $m_V = 7.1$. It was possible to rule out a spherical geometry for the wind of AB Aur and provide realistic solutions to account for the Hα emission compatible with magneto-centrifugal acceleration. It was difficult, however, to determine the exact morphology of the wind because of the surrounding asymmetric nebulosity. The study illustrates the advantages of optical interferometry and motivates observations of other bright young stars in the same way to shed light on the accretion/ejection processes.

Key words. Methods: observational Techniques: high angular resolution - Techniques: interferometric - Stars: individual (AB Aur) Stars: emission-line - Stars: circumstellar matter

arXiv:1005.5267v1 [astro-ph.SR] 28 May 2010

1. Introduction

The class of Herbig Ae/Be (HAEBE) stars gathers the pre-main-sequence stars of intermediate mass ($1.5 \leq M/M_{\odot} \leq 10$), with spectral types of B to F8, strong emission lines, and the presence of infrared to submillimeter excess flux. Like their solar-type analogs, the T Tauri objects, HAeBe objects are known to be surrounded by protoplanetary disks of gas and dust, responsible for this excess emission. In the case of lower mass stars, the formation is commonly explained by the gravitational collapse of a dusty disk cloud and magnetically controlled accretion via a disk. The formation of more massive stars is still very uncertain. However, determining if similar processes are at work in these objects is extremely important, as it would help to establish whether the accretion/ejection mechanism is universal irrespective of the mass of the central body. The hot gas that can be involved in accretion and ejection flows close to the source and can be used to probe the corresponding physical conditions through its emission in lines, especially those in the optical range that have a high diagnostic potential. These phenomena, however, occur in a small region of a few astronomical units (AU) around the star, corresponding, for close star formation regions, to a few milliseconds of arc. Such a small scale can only be resolved with interferometry.

Send offprint requests to: Karine.Perraut@obs.ujf-grenoble.fr

Guided by these considerations, we have attempted for the first time to observe a bright visible Herbig Ae/Be star, AB Aurigae, with a spectro-interferometer operating at optical wavelengths, the VEGA spectrograph (Mourard et al. 2009) installed at the CHARA Array (Brummelaar et al. 2005). This unique combination of spectral and spatially resolved information allowed us to study the physical conditions for the gas producing the Hα line on sub-AU scales. Interpreting the results, however, required appropriate modeling of the emitted radiation. Using a radiative transfer code, we obtained observational insights on the generation mechanism of winds around AB Aurigae, giving experimental support to the widely accepted, but not yet tested, theory of magneto-centrifugal acceleration. In Sect. 2, we recall the present knowledge about the target. In Sect. 3, we describe the observations and the data processing. In Sect. 4, we present the radiative transfer code and discuss the wind models adopted to interpret the observed Hα visibilities and spectrum.

2. The target: AB Aurigae

AB Aurigae (AB Aur; A0Ve; d=144 pc) is the brightest Herbig Ae star in the northern hemisphere, and is often considered as the prototype of the HAeBe class. Its photometric and spectral properties are well studied over a wide wavelength range (Böhm & Catala 1993, Catala et al. 1999, Grady et al. 1999a, Van den Ancker et al. 1999) and there is evidence of both accretion and outflows in AB Aur (Catala & Kunasz 1987, Garcia-Lopez et al. 2006, Wassel 2009). The Hα line exhibits a P-Cygni profile, which is a common probe of stellar wind, and is known to be variable, especially in the blue wing of the line. Among the alternatives evoked to explain the observed variability were a wind coming either from the equatorial regions of the star or from a circumstellar rotating disk (Catala et al. 1999). The wind in AB Aur seems to be complex, probably controlled by a magnetic field, even if no magnetic detection of AB Aur has been reported so far (Alecian et al. 2007).

AB Aur is surrounded by a complex combination of gas-rich and dust-dominated structures probed on large scales by imaging. Using the HST, Grady et al. (1999b) detected extended nebulosity and circumstellar material at all position angles out to 1320 AU in the R-band, whereas Fukagawa et al. (2004) detected a double spiral structure at 200-450 AU in the H-band. Spatially resolved observations at high angular resolution at near-infrared, thermal infrared, and millimetric wavelengths have shown the presence of a circumstellar disk (Millan-Gabet et al. 2001, Eisner et al. 2004), rotating at non-Keplerian velocities (Piétu et al. 2005). All these observations agree on a low inclination for the system (i.e., i≤40°), in disagreement with the value of 70° ± 20° deduced from spectroscopic studies (Catala et al. 1999). A strong near-infrared continuum emission was found inside the silicate dust sublimation radius (0.24 AU) and was interpreted as due to a hot gaseous disk (Tannirkulam et al. 2008). A localized asymmetry on spatial scales of 1-4 AU has also been detected by Millan-Gabet et al. (2006) who speculated that it might result from either localized viscous heating due to a gravitational instability in the disk or from a close stellar companion, in agreement with spectro-astrometric observations in the optical lines (Baines et al. 2006).

3. Observations and data processing

Data were collected at the CHARA Array with the VEGA spectrometer recording spectrally dispersed fringes at visible wavelengths. Two pairs of telescopes were combined: W1W2 (whose projected baseline B∼100 m) and S1S2 (B∼34 m). Observations were performed around the Hα line, between 610 and 700 nm, at the lowest spectral resolution of VEGA (R=1700). Observations of AB Aur were sandwiched between those of a nearby calibration star (HD 29646) that was chosen to be bright enough (m_V = 5.7) and to have a similar spectral type (A2). The observation log is given in Table 1.

Table 1. Journal of AB Aur observations on October 8 and 9, 2008.

Date	UT	Star	B (m)	PA (°)	HA
2008-10-08	09:45	HD 29646	33.9	1.66	-1 h 27
2008-10-08	10:05	AB Aur	34.0	0.98	-1 h 22
2008-10-08	10:24	HD 29646	33.9	-4.02	-0 h 47
2008-10-08	10:45	AB Aur	34.0	-4.94	-0 h 40
2008-10-09	08:21	HD 29646	86.1	120.9	-2 h 32
2008-10-09	08:57	AB Aur	89.9	119.4	-2 h 32
2008-10-09	09:25	HD 29646	95.8	112.0	-1 h 43
2008-10-09	09:49	AB Aur	99.0	110.3	-1 h 25

Each set of data was composed of observations following a sequence calibrator-star-calibrator, with 10 files of 3000 short exposures per observation. Each data set was processed using the C_1 estimator and the VEGA data reduction pipeline detailed in Mourard et al. (2009), with a large spectral band of 20.4 nm (shifted by steps of 10.2 nm over the observing range) to reach a sufficient signal-to-noise ratio. The resulting resolution of the spectral visibilities is R=30, leading to an interferometric field of view of 240 mas. The poor signal-to-noise ratio meant that the visibilities could not be processed for the data recorded with W1W2. Only the squared visibilities corresponding to S1S2 were computed in 9 spectral channels and calibrated using an angular diameter of 0.20±0.01 mas for the calibrator HD 29646[1] (Fig. 1-right).

The VEGA spectrum of AB Aur exhibits an Hα emission line with a clear P-Cygni profile (Fig. 1-left). The line to continuum ratio is at most about 2.5, the line FWHM is 6 Å, and its emission peak is slightly red-shifted. In addition, the line presents a very broad absorption from ∼640 nm until ∼665 nm, probably due to Stark broadening in the absorption of the radiation by nearly hydrostatic cold layers located just above the star's photosphere (Felenbok et al. 1983). Due to the width of the processing spectral window, the squared visibilities at 646 nm, 656 nm, and 666 nm include all or part of the Hα emission, and the values of the squared visibility are between 0.72 and 0.75. Although they are relative to continuum emission alone, the squared visibilities at 636 nm and 676 nm are below unity, while those farther away from Hα are consistent with 1. AB Aur is thus clearly resolved by the S1S2 baseline both in the Hα line and in a part of the visible continuum.

4. Modeling and discussion

The spectroscopic P-Cygni feature in AB Aur shows that the line is formed at least in part in a wind. Therefore, we focused on a wind model to constrain the properties of the emitting region. To simultaneously reproduce both the line profile and the spectral visibilities, we have adapted two numerical codes in spherical symmetry for the production and transport of hydrogen (H) lines (Rajabi 2010). The first one, RAMIDUS, calculates the level populations of H in a moving fluid for assigned

[1] http://www.jmmc.fr/searchcal_page.htm

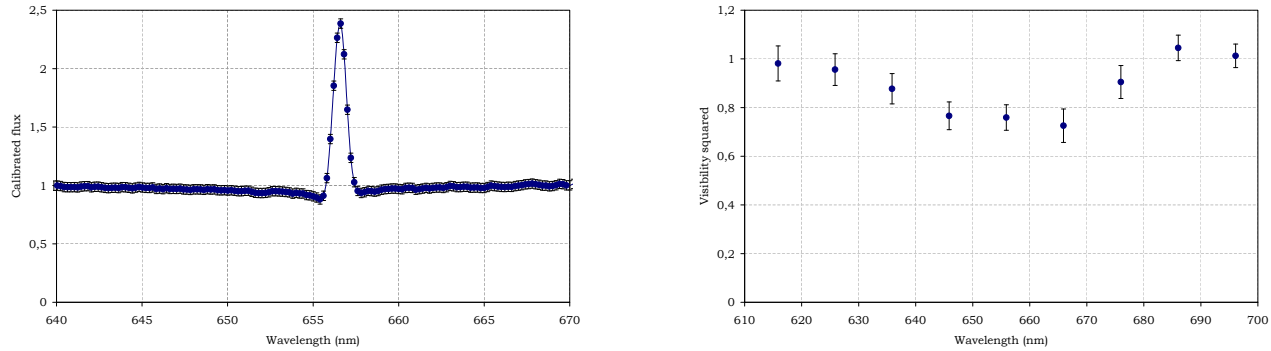


Fig. 1. Left. Hα line recorded at R = 1700 with VEGA. **Right.** Calibrated squared visibility at R = 30 obtained with the S1S2 CHARA baseline.

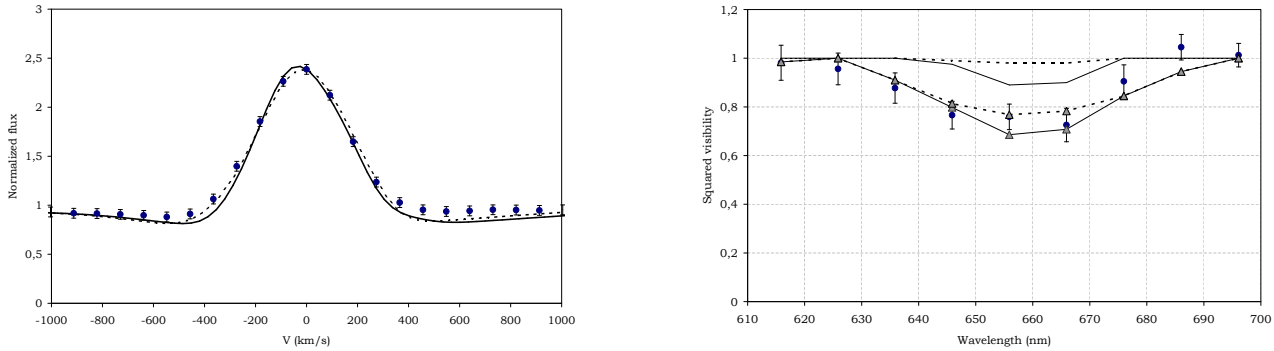


Fig. 2. Best model predictions compared to the VEGA spectrum (left) and spectral visibilities (right), both in full circles with error bars. Dashed lines correspond to the X-wind model and full lines to the disk-wind one. For the squared visibilities, triangles denote the model prediction including both the wind and the contribution of the asymmetric reflection nebula.

radial dependencies of the basic wind parameters (density, velocity, temperature). The code uses the Sobolev approximation and the escape probability method (Castor 1970). In cascade, the PROFILER code calculates synthetic images, line profiles and visibilities of H lines for various geometrical configurations. By selecting limited portions of the spherical winds, we approximated 2-D axisymmetric models. We did not include accretion in the models.

A full spherical wind providing matter along the line of sight can be readily excluded, because it would produce too much blue-shifted absorption with respect to the observed P-Cygni feature that is shallow but not very deep (normalized flux$\geq$0.88). Even if the issue of the inclination angle of the AB Aur system is still alive (see Sect. 2), we chose a wind geometry in agreement with a small inclination (i$\leq$ 40°), and thus excluded a double cone geometry, reminiscent of a bipolar jet, which would lead, for small inclinations, to a line profile with two distinct emission features instead of the observed single peak. Inspired by the magneto-centrifugal (MC) scenario for the acceleration of stellar jets, we assume that, on the observed scales (much less than 2-3 AU from the star/disk), the wind occupies a region delimited by a flattened torus defined by the pale gray region in Fig. 3. This configuration can simulate the base of either a X-wind (Camenzind 1990, Shu et al. 1995) or a disk-wind (hereafter D-wind; Ferreira 1997, Konigl & Pudritz 2000) accelerated along the magnetic field lines anchored in the inner few AU of the accretion disk. In this region the wind has a wide angle aperture, as it has not yet reached the Alfvèn surface, after which magnetic collimation occurs and the wind collimates into a jet. In Fig. 3, R_i=0.02 AU is the corotation radius, R_d=0.24 AU is the inner radius of the optically thick dusty disk, R_f=2.3 AU is the extension of the wind, and α is the angle between the disk mid-plane and the surface of the wind, constrained to be $\leq 60°$ for MC acceleration to occur (Spruit 1996). In our X-wind model, all the material in the flow comes from the region located very close to the corotation radius and has a constant mass outflow rate $\dot{M}_w$ through the torus section, while for the D-wind $\dot{M}_w$ progressively increases from R_i to about 1 AU, to simulate that the wind originates in an extended region of the disk. The wind velocity is assumed to be $V(r) = V_0 + V_f(1 - (R_\star/r)^2)$, where V_0 = 20 km.s^{-1} is the initial velocity, r the radial distance from the star, $R_\star$ the stellar radius, and V_f the terminal velocity. The density profile is dictated by $V(r)$ and $\dot{M}_w(r)$ through the mass continuity

Table 2. Parameters of the models, with $N_{H,ej}$ the average hydrogen density at the wind footpoints.

Model	i	α	V_f [km/s]	$\dot{M}_w$ [$M_\odot$/yr]	$N_{H,ej}$ [cm^{-3}]
X-wind	0°	60°	410	3.7 10^{-8}	4.3 10^{10}
D-wind	20°	35°	450	2.2 10^{-7}	7.7 10^{8}

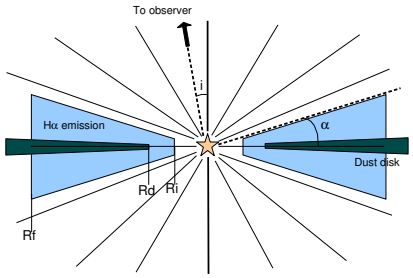


Fig. 3. Geometry adopted for the empirical X-wind and disk-wind models described in Table 2. R_i, R_d, and R_f are the corotation radius, dust sublimation radius, and extension of the wind, respectively.

equation, while the gas temperature profile T(r), which reaches a maximum of 12 000 K, is chosen in accordance with the theory of wind heating illustrated by Shang et al. (1998) and Garcia et al. (2001) for the X-wind and D-wind, respectively. Modeling of the Stark absorption in the extended line wings has been included using a template spectrum from Kurucz (1979).

Regarding the modeling of the line profile, both an X-wind and a D-wind could provide a good fit (Fig. 2-left) for the model parameters collected in Table 2. To reproduce at the same time the line width and the absence of a strong blue-shifted absorption, the best predictions for the X-wind have nearly a null inclination (i) and a large opening angle (α) of 60°. For the D-wind model, since the disk hides part of the high velocity material in the red-shifted wing, the best predictions are obtained with a small inclination (20°) and a smaller opening angle of 35° to avoid too much blue-shifted absorption. Both models lead to a small inclination in agreement with the previous interferometric determinations. As pointed out by Pogodin (1992), a change in the opening angle of the wind (α) affects the depth of the blue-shifted absorption. Concerning the mass loss rate $\dot{M}_w$, our best prediction is of the same order as previous determinations from line profile analysis (Catala & Kunasz 1987) for the X-wind but is significantly higher for the D-wind. In fact, our various simulations clearly show that the estimate of $\dot{M}_w$ is very dependent on the velocity law and the temperature profile considered in the wind model, and on the scale on which the wind is accelerated. Since the geometry of our D-wind model strongly deviates from a spherical wind, the value of $\dot{M}_w$ obtained for this model cannot be directly compared to the previous determinations of $\dot{M}_w$.

Regarding the modeling of V^2, the X-wind provides only a negligible decrease in Hα (V^2 = 0.98) with respect to the continuum (Fig. 2-right). In this case, the emission is concentrated at R_i, while it is much more extended in the D-wind model that produces a larger decrease in V^2 (down to 0.89). In both cases, however, the observed visibility variation could not be modeled with the wind alone so we considered an additional component producing an extended continuum emission. This component could come from the extended reflection nebulosity around the system, already reported by several authors (Grady et al. 1999b, Fukagawa et al. 2004, Millan-Gabet et al. 2006). In practice, we used this secondary source to reproduce the modulation of the visibility in the continuum. Our wind models combined with this additional emission provided a good fit of the visibilities. For instance, Fig. 2-right corresponds to a secondary source separated from the star by 38.2 mas (i.e. 5.5 AU) contributing to 7% of the total flux. Because of the large number of free parameters and the fact that we only have measurements along one baseline direction, we found many different configurations for the secondary emission that could fit, for both wind models, the observed visibilities (e.g. a much larger separation of 591.2 mas).

In conclusion, thanks to the unique capabilities of VEGA/CHARA, we managed for the first time to record simultaneously a spectrum at a resolution of 1700 and a visibility spectrum in the visible range on a target as faint as m_V = 7.1. Despite the limited signal-to-noise ratio of our data, they allowed us to rule out a spherical wind and to make realistic predictions on the nature of the Hα emission region at sub-AU, and our data are compatible with a magneto-centrifugal mechanism for the production of the wind. It was difficult, however, to determine the exact morphology of the wind and disentangle the X-wind and the D-wind because of the extended nebulosity. Moreover, all models neglect the contribution of mass accretion to the H-line emission, so self-consistent models of winds including this process are needed. Complementary observations with larger CHARA baselines are required to place more stringent constraints on the complex environment and the photosphere contribution of AB Aur that can be resolved in the visible with VEGA. We also expect to take advantage of the new instrumental facilities of CHARA to study other bright HAeBe and provide promising insights on the accretion/ejection mechanisms in intermediate-mass young stars.

Acknowledgements. VEGA is a collaboration between CHARA and OCA-LAOG-CRAL-LESIA supported by the French programs PNPS, ASHRA, by INSU, by the Région PACA, and by the OCA and CHARA technical teams. The CHARA Array, operated by Georgia State University, was built with funding provided by the National Science Foundation (NSF), Georgia State University (GSU), the W. M. Keck Foundation, and the David and Lucile Packard Foundation. Array operations are supported by NSF (grant AST0606958) and by the office of the Dean of the College of Arts and Science at GSU. M.B. acknowledges funding from INAF (grant ASI-INAF I/016/07/0). S.R. acknowledges funding from European Community FP6 (MCRTN 005592) and FP7 (GA 226604). We warmly thank the referee whose comments helped us clarify some important issues. We thank C. Giovanardi and P. Garcia for fruitful discussions. This research has made use of the SearchCal service of the Jean-Marie Mariotti Center and of CDS Astronomical Databases SIMBAD and VIZIER.

References

Alecian, E., Wade, G.A., Catala, C. et al., 2007 SF2A proc., 431
Böhm, T., Catala, C. 1993, A&AS, 101, 629
Baines, D., Oudmaijer, R. D., Porter, J.M. 2006, MNRAS, 367, 737
ten Brummelaar, T. et al. 2005, ApJ 628, 453
Camenzind, M., 1990, Reviews in Modern Astronomy, 3, 234
Castor, J., 1970, MNRAS, 149, 111
Catala, C., Donati, J.F., Bohm, T. et al. 1999, A&A, 345, 884
Catala, C., Kunasz, P.B. 1987, A&A, 174, 158
Eisner, J. A., Lane, B. F., Hillenbrand, L. A. et al. 2004, ApJ, 613, 1049
Ferreira, J. 1997, A&A, 319, 340
Felenbok, P., Praderie, F., Talavera, A., 1983, A&A, 128, 74
Fukagawa, M., Hayashi, M., Tamura, M. et al. 2004, ApJ, 605, L53
Garcia P.J.V. 2001, A&A, 377, 589
Garcia Lopez, R., Natta, A., Testi, L., & Habart, E. 2006, A&A, 459, 837
Grady, C. A., Pérez, M.R., Bjorkman, K.S. et al. 1999a, ApJ, 511, 925
Grady, C. A., Woodgate, B., Bruhweiler, F.C. et al. 1999b, ApJ, 523, L151
Konigl, A., Pudritz, R., 2000, PPV
Kurucz, R.L. 1979, ApJS, 40, 1
Millan-Gabet, R., Schloerb, F.P., Traub, W.A. 2001, ApJ, 546, 358

Millan-Gabet, R., Monnier, J.D., Berger, J.P. et al. 2006, ApJ, 645, L77
Mourard, D., Clausse, J.M., Marcotto, A., et al. 2009, A&A, 508, 1073
Piétu, V., Guilloteau, S., Dutrey, A., et al. 2005, A&A, 443, 945
Pogodin, M.A. 1992, SvAL, 18, 437
Rajabi, S. 2010, PhD thesis, University of Porto, Portugal
Shang, H., Shu, F.H., Glassgold, A.E. 1998, ApJ, 493, L91
Shu, F.H., Najita, J., Ostriker, E.C., Shang, H. 1995, ApJ, 455, L155
Spruit, H.C. 1996, NATO ASI Series C, Vol. 477, 249-286
Tannirkulam, A., Monnier, J.D., et al. 2008, ApJ, 689, 513
Van den Ancker, M.E., Volp, A.W., Pérez, M.R., De Winter, D. 1999, IBVS 4704
Wassel, E., J. 2009, PhD thesis, Catholic University of America, USA